DETECTION OF SPACE DEBRIS BY THE USE OF SPACE BASED OPTICAL SENSORS+

J. Bendisch*, J. P. Hoffmann**, R. Liebscher□, F. Rollenhagen□□

*Institut für Raumflugtechnik und Reaktortechnik (IFRR), Technical University of Braunschweig, Germany
Deutsche Aerospace (DASA), **ERNO Raumfahrttechnik GmbH, Bremen, Germany,□Jena Optronik GmbH, Jena, Germany
□□ DLR, Institut für Weltraumsensorik, Berlin, Germany

ABSTRACT

A number of space programs, especially those, which include manned activities, have to deal with safety problems which are posed by the natural and man-made space debris environment. Hence, it is of major interest to close the existing data gap in the object size region between 1 cm and 10 cm in diameter. Besides existing and planned ground based facilities, space based sensors may contribute substantially to fill the a.m. data gap. This paper addresses the requirements for optical space based systems and their missions. Technical solutions and mission parameters, which are applicable and feasible, are discussed. A preferable concept is presented which seems to be capable to get a first in situ impression of the actual space debris environment between 1 cm and 10 cm. Such a mission can be performed soon and could be the basis for a more advanced space based debris sensor.

1. INTRODUCTION

During the last years it has become a fact, that the issue of orbital debris has to be taken into account in a number of space programs. Due to the high relative velocities occurring during a collision even small particles are posing a non-negligible risk for operating spacecraft. Costly protective measures like shielding and collision avoidance may reduce this individual risk for a specific mission on the short and mid term. On the long term a significant change in orbital operations will be necessary in order to establish effective debris mitigation procedures. A number of remarkable international activities as well as the rapid growth of the number of articles in the relevant literature are giving rise for this cognition. But indeed all current activities are based upon the insufficient knowledge of the actual number and orbital distribution of debris. Only the app. 7,000 catalogued objects larger than about 10 cm are more or less deterministicly known, below that size regime debris models have been established (Refs. 1,2), which include a number of sporadic measurements in the mm and sub-mm size region, e.g. those provided by spacecraft (Ref. 3) that have been retrieved to earth. These models allow for the analysis of the present object flux as well as for predictions of the future space debris population. But although a lot of sophisticated work has been done, these models are in need for validation, since they are effected by a broad band of uncertainties. As long as these uncertainties cannot be reduced sufficiently it will be very difficult to establish debris minimization and mitigation measures within the space flight community, even if a number of results of the debris analysis so far indicate the need for such actions in spite of these uncertainties. A first significant approach in order to close the a.m. data gap in the 1 cm to some dm size regime are the measurements carried out by the Haystack ground radar (Ref. 5). Additional measurements will be necessary to deal with all uncertainties in the current state of space debris modeling and to support the measurements carried out by the Haystack radar, since this system will not provide a catalogue of objects smaller than 10 cm comparable to the existing USSPACECOM catalogue. Space based optical sensors may have the capability to provide additional information on the actual space debris environment beyond some limitations of ground based systems.

2. REQUIREMENTS

2.1 Basic goal

The major requirement for space based optical debris sensors is to provide data that can be implemented into the existing space debris models for the purpose of validation. Fig. 1 illustrates the interaction between the current model and additional measurements. As can be seen from Fig. 1 the development of a space based sensor is effected by the existing space debris models which provide the theoretical basis for the prospected performance of such a system.

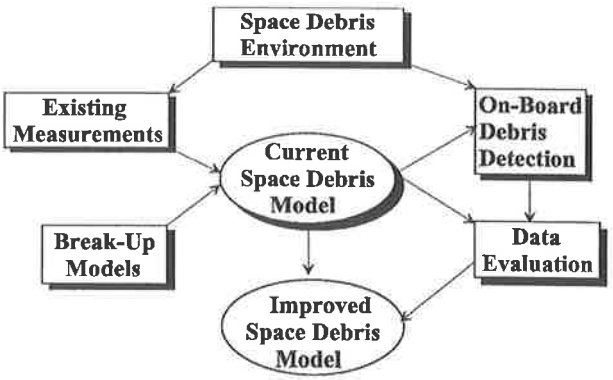

Figure 1. Space Debris Model Validation

+The work presented in this paper was carried out under a contract of the German Space Agency DARA (FKZ 50 IP 9157 1991/92)

2.2 Debris optical characteristics

The basic requirements and influences for an optical space based debris sensor are given in Fig. 2.

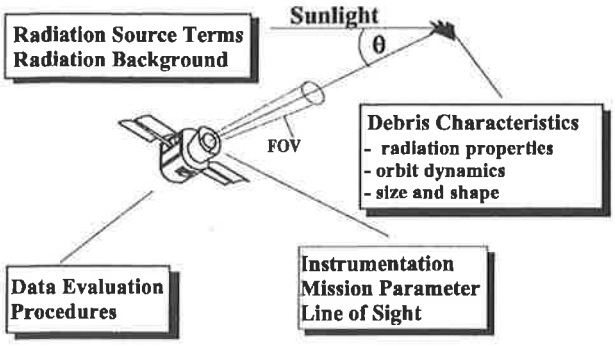

Figure 2. Requirements for a space based debris sensor

For the sake of simplicity in system evaluation small debris particles are normaly approximated as "grey", perfectly scattering Lambertian spheres. In this case the resulting bond albedo is a function only of the total reflectance of the objects surface and the phase angle (cf. Fig. 2) between the debris-sun direction and the optical axis of the telescope. This assumption, however, is subject to modifications if a stable flying circular disk is more appropriate, as in most real cases. For comparison, the incoming radiation (at the entrance plane of a telescope) can be written as in Eq. 1.

Since most of the objects might not be spheres, but rotating irregular formed bodies, plates and bars, the individual effective surface of the objects has to be reduced. The effective phase angle under which an object is seen strongly depends on the telescope alignment with respect to the orbital plane and the actual sun declination (second order, launch time impacts). The phase angle can be optimized, if the objects appear in the field of view of the sensor like full moons (phase angle = 0°), e.g. using sun-synchronous orbits in the vicinity of the day-night terminator and the line of sight directed anti-solar (i.e. normal to the orbital plane).

$$H_{T_S} = \frac{2\, E_{S_\lambda}\, \rho_A\, r_D^2\, (\sin\theta + (\pi - \theta)\cos\theta)}{3\, \pi\, R^2}$$

$$H_{T_D} = \frac{E_{S_\lambda}\, \rho_A\, r_D^2\, \sin\phi\, \cos\theta}{R^2} \qquad (1)$$

where,
H_{TS}= incoming radiation released by a Lambert. sphere
H_{TD}= incoming radiation released by a circular disk
r_D = debris object diameter; R = range sensor- debris object
θ = phase angle; ϕ = slant angle (90 deg ≙ vertical plate)
ρ_A = debris object albedo;
$E_{S\lambda}$ = solar irradiance = 1350 W/m²

The albedo of the objects is not known individually. From measurements (Ref. 6,7) carried out so far concerning objects larger than 10 cm a statistical albedo distribution can be derived, indicating that most of the objects have an albedo < 0.1. The albedo distribution however is broadly spreaded.

2.3 Radiometric Conditions

In a conservative estimate, the following radiative intensities have been derived: With 60% spectral sensitivity of a CCD in the range of 400 nm to 1000 nm wavelength, a particle under zero phase angle and 10% average albedo exhibits a radiation density of E_λ =26 W/m²sr. The incident radiation at the entrance plane of a telescope in a distance of 100 km yields not more than $2*10^{-13}$W/m² for a 1 cm particle. With a slightly defocused image spot on two pixels and with an optics transmission factor of 0.75 the resulting radiation intensity on a single pixel is $E_{pixel}=4.1*10^{-8}$ ....$3.3*10^{-6}$ W/m² for a 70 mm and 200 mm aperture, respectively.

Obviously, with such small intensities any stray light or scattered radiation from discrete sources (atmospheric reflections, milky way, sun, moon, bright stars) has to be prevented by design measures on the telescope and by considering operational mission constraints. The latter are to be considered anyway because a certain level of continuous radiation cannot be avoided due to the many stars which are always in the background. Near the ecliptic plane reflected sun light from cosmic dust and particle clouds create the so called zodiacal light as a diffuse foreground light source of varying intensities.

Fig.3 shows the corresponding isophotes S_{10} in terms of the equivalent number of stars N_{S10} of the 10th (visual) magnitude for a mid March sun/moon constellation. The highest isophotes delineate S_{10}=1000 and the S_{10}=150 contour opposite to the sun roughly defines the antizodiacal light. Also indicated in Fig. 3 are regions on the celestial sphere with high background light such as the milky way and the constrained viewing angles around the sun (up to 50°) and the full moon (15°). These disturbing backgrounds, however, can be controlled in short term experiments by means of an appropriate seasonal launch window.

The star background cannot be avoided and provides a quasi-continuous background radiation. Although there is some variation in the average irradiance level over the galactic latitude for the purpose of system evaluation a constant diffuse radiation with an intensity equivalent to 200 stars of the 10th magnitude per square degree is taken.

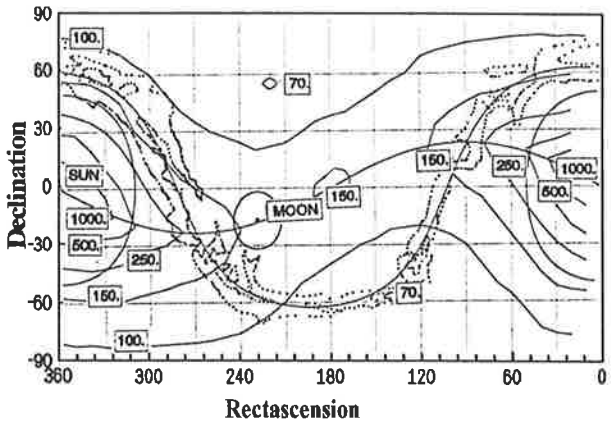

Figure 3. Zodiacal background (total sky) on March 21st including constraints (sun, moon, milky way)

2.4 Optical parameters

The difficult radiometric conditions in debris detection require an optimization between the optical parameters of the telescope and the performance characteristics of the selected CCD matrix.The background noise which is actually accumulated on pixel level depends primarily on the focal ratio and the integration time. Sufficiently high SNR basically requires a large telescope aperture in conjunction with a relatively small field of view. Fig. 4 shows the possible improvement in debris detection capability for a refractor system if the entrance diameter is enlarged and the focal ratio is reduced. The FOV is 3°, as compared to 10° in the original concept. In both cases a highly sensitive CCD with an effective size of 11x7mm is presumed. About the same performance can be achieved with a larger matrix (28x26mm) by applying a Schmidt reflector telescope. The refractor system (R-Intensar) given in Fig.5 is space qualified and availabe at JENA OPTRONIK.

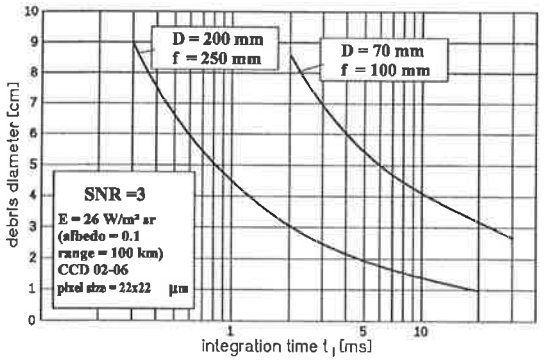

Figure. 4 Detectable debris size as function of integration time, aperture (D) and focal length (f)

3. ENCOUNTER SCENARII

3.1 Observation simulation

The encounter scenarii describe the angular distribution, the angular velocity and radial/angular acceleration as well as the total number and the duration of the encounters of objects passing the field of view (FOV) of a space based sensor.

The a.m. parameters are determined by the dynamic of the mission orbit and the modeled debris environment. Simulations have been carried out at IFRR in the frame of the reference feasibility study (Ref. 8), using the IFRR debris model (Ref. 2) and a deterministic simulation software. The sensor parameters have been considered in terms of a given nominal sensitivity, since, to the first order, $R_{max} \sim r_D$ (Eq. 1). This procedure represents some kind of a realistic preselection of objects in order to reduce the amount of data during the simulations. The scenarii were described omni-directional as a function of mission parameters and, in a next step, as a function of line of sight direction and FOV. They are used to evaluate the performance of a given sensor and of the selection effects introduced. The calculations have been performed for preferable mission types:

- 300 km - 400 km alt., circular (manned spaceflight)
- app. 800 km alt., circular, sun-synchronous (max. object density, source of future object flux at lower altitudes, collision cascading may set in)
- 400 km x 800 km, elliptical, sun-synchronous.

These types correspond with potential flight experiment opportunities on the STS-Orbiter, MIR1-Station modules as well as remote sensing satellites and 100° (sun-synchronous) inclination. Fig. 6 illustrates some selection effects with respect to the inclination distribution of the debris model.

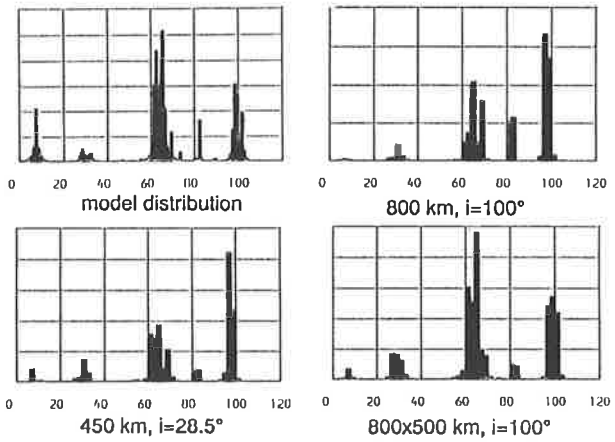

Figure 6. Inclination distribution of objects encountering a sensor on various orbits (omni-directional sphere)

concept	aperture D	f/D	f [mm]	FOV[°]	CCD	no. of pixels
Schmidt	200 mm	3	600	3	EEV 05-30	1242 x 1152
Intensar	70 mm	1.4	100	10	EEV 02-06	500 x 320

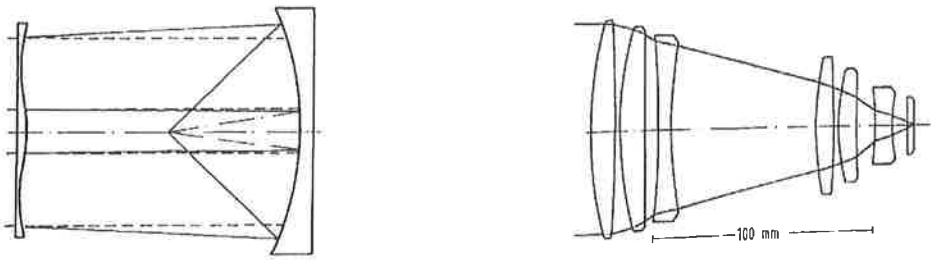

Schmidt Telescope

R-Intensar Telescope

Figure 5. Proposed optical concepts for an in-orbit experiment

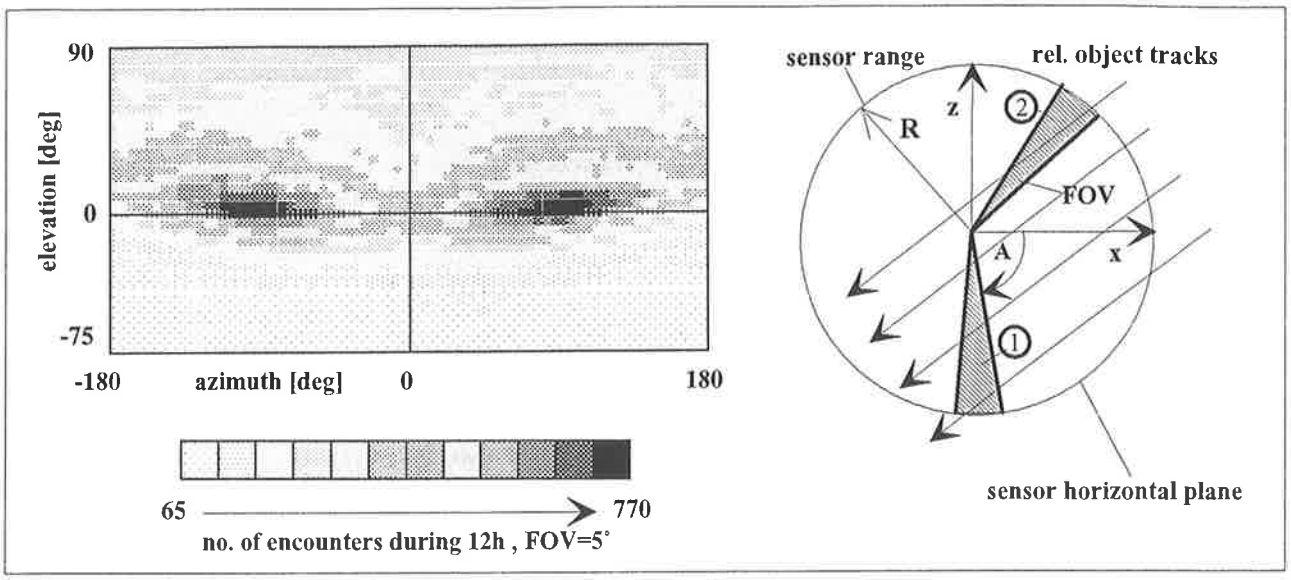

Figure 7. No. of encounters during 12 h within a FOV of 5° as function of LOS direction (sensor orbit 800 km, sun-synchronous)

Another example is given in Fig. 7, where the number of encounters within a FOV of 5° per time unit are plotted versus azimuth and elevation in a sensor fixed coordinate system (local horizontal plane, x = flight direction). For this example a max. range of 100 km was assumed for 1 cm sized objects (sensor orbit 800 km, sun-synchronous). It can be seen from Fig. 6, that most of the encounters occur within the horizontal plane (E=0°) and perpendicular (A=±90°) to the flight of the sensor. If the line of sight (LOS) is viewing into this direction (A=+90°), the optimum object illumination is provided, since for this orbit the sun appears at A=-90°.

Fig. 7 (diagram on the right) also shows that, due to the specific angular distribution of the object flux (Ref. 1,2), the line of sight direction not only has an effect on the encounter rate but also on the encounter duration and directionality. The arrows in Fig. 7 represent one half of the main object flux within the horizontal plane. A FOV looking into that main flux direction (2) would see less objects than FOV (1), but the objects could be detected longer.

3.2 Detection simulation

Computer simulations are a valuable tool for the purpose of design and mission planning of in-orbit detection experiments. At DASA/ERNO existing standard mission analysis software tools have been extended for debris detection simulation.

Based on the observation data bases as for instance drawn from the IFRR debris population model detailed imaging simulations can be performed for a specific FOV and the inherent optical parameters of a projected telescope. The move of the FOV over the celestial sphere can be shown for the different orbits and the varying orientations of the optical axis. Fig. 8 exemplifies results to be gained from a detection simulation for a sun-synchronous orbit of 800 km altitude. The object is on a slightly elliptical orbit with an inclination of 65°. The pass time through the FOV is around 1 second and the corresponding pixel dwell time in the focal plane is 0.9 milliseconds. With certain assumptions about the radiative properties of the debris object radiometric evaluations are feasible. For background radiation assessments an interpolation procedure over the FOV on the celestial sphere has been introduced. For this purpose maps of the constant intensity lines (isophotes) in celestial coordinates have been tabulated representing average star radiation and zodiacal light (Fig. 3) in terms of stellar magnitudes of the visible band. These intensities in conjunction with the actual position of the FOV relative to the constrained areas around the sun, the moon and the milky way are determined for the preferable LOS-orientation and experiment launch date to be selected.

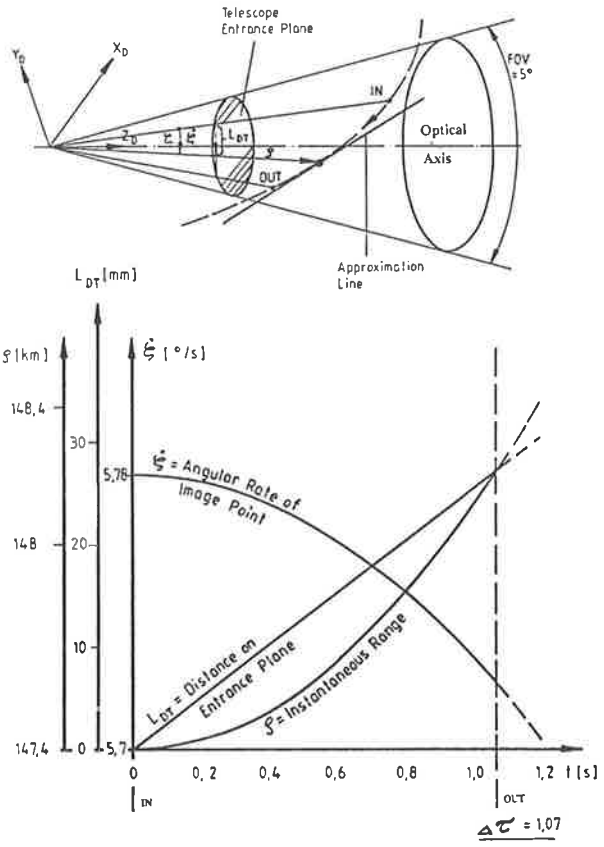

Figure 8. Example of a debris detection at 800 km, sun-sync

Fig. 9 depicts the isophotes of visual star radiation over the celestial sphere with the sun/moon position for the winter solstice. The detector's FOV is indicated for a 450 km orbit with i=28.5°, looking vertical away from the sun. Parametric investigations of the illumination/detection situation are mandatory in order to guarantee as many as ever possible debris encounters.

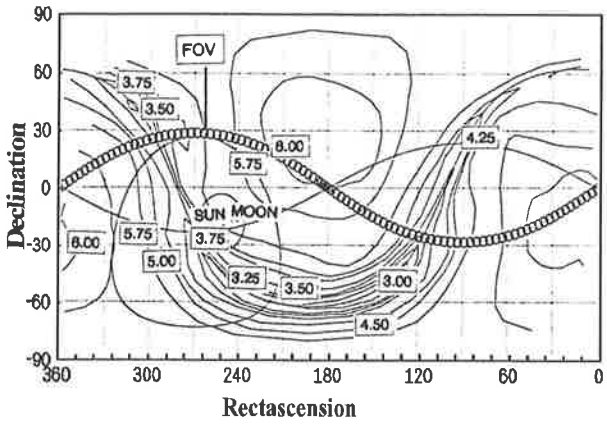

Figure 9. Visible star background on 21.12.95, FOV(o)=5°, Orbit 450 km, i=28,5°, LOS A=0, E=90°

Fig. 10 compiles the relationship between the detection range and the dwell time of the sharp debris image on a small pixel. The detector has a FOV of 5° and could be mounted on a space platform in LEO. The figure shows twofold:

• The lower limit of the detection range will be determined by the readout frequency of CCD matrix and the acceptable defocusing of the debris image point. With an assumed minimum dwell time of 0.5 ms the smallest particle can be seen in a distance of 10 to 60 km from the detector, depending on the relative velocity.

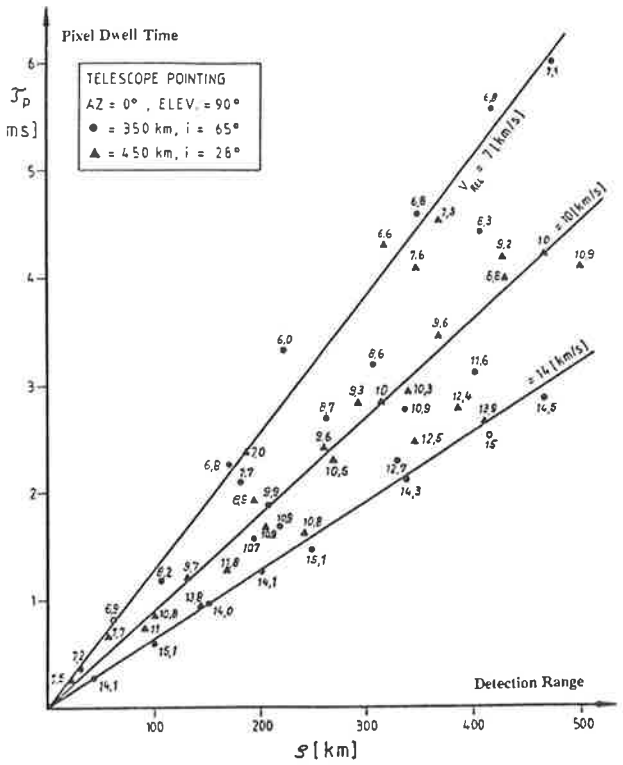

Figure 10. Pixel dwell time as function of range debris/sensor

• The detector may selectively see more of the bigger objects in larger distances where the more crowded debris populations reside. However, due to the slower angular rates with large dwell times, not enough pixels may be saturated during the exposure time for the required digital image processing (cf. section 4.2). Also, to limit background disturbances the pixel dwell time must not exceed a system typical value. Due to this constraints an upper range limit of 300 km might be realistic.

4. DATA ACQUISITION AND IMAGE PROCESSING

4.1 Data evaluation

There are several levels of alternate data evaluation procedures leading to specific sensor requirements. If only the actual flux of objects within a certain altitude band, regardless of object size and orbital parameter like inclination and eccentricity, is of major interest a sensor only would have to operate as a simple event counter. This would require the capability of detection anything that is moving in the vicinity of the sensor and within its field of view. A next step is to require that also the object size distribution within 1 cm to 10 cm in diameter can be determined. Such a capability is of major interest in the frame of space debris model improvement. Hence, this requirement (i.e. to measure the absolute irradiance of an object and its range and to determine its size subsequently according to Eq.1) should be the baseline for the sensor system design. Hence, the number of detections needed for a significant improvement of the existing debris models has to be evaluated. Taken into account the uncertainties of the measured irradiance and range of an object and of its statistical albedo scattering, the absolute number of detections required to derive a statistical relevant size distribution can be found as in Fig. 11.

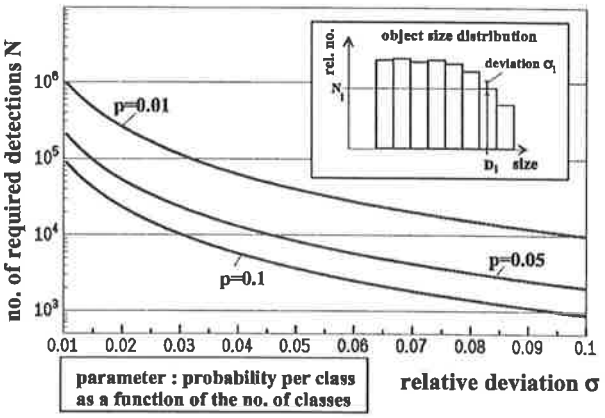

Figure 11. Number of required detections as a function of the resulting object size distribution accuracy

4.2 Aspects of image processing

Due to the radiometric situation an optimization process between the optical system and the attached electronic chain is advisable. However, if space qualified hardware is available, very often, due to project constraints optimization can only be attempted on the software side. The goal is to investigate possible image processing procedures which are feasible with currently available, space qualified components.

Also, when aiming on short term flight opportunities for an experimental debris detector, a high degree of autonomy should be provided. An accelerated data evaluation and compression process must be provided on-board in order to limit the telemetry rates and/or the required recording capabilities. The compressed data are to be evaluated on the ground. The following steps are proposed for the on-board signal processing and data evaluation procedures:

- Sensor calibration based on stellar coordinates and radiation characteristics of selected stars
- Initial identification and radiometric calibration of the debris signal
- Prediction of the potential track continuation region and generation of readout masking for the next exposure
- Accurate determination of the matrix coordinates for the moving SD-images and for selected reference stars on the time-tagged consecutive frames
- Data compression and storage (dedicated RAM or tape)

Fig. 12 shows the functional diagram of the related sensor electronics. The gating signal for the image intensifier is generated in a timing and clock generator which also delivers the signal for the CCD. Digital data processing starts with radiometric calibrations including an offset correction and background noise evaluation in order to generate a signal threshold for the digital computer. Based on this criteria a binary picture is generated and stored in the dedicated shift register. The results of the validity checks for 16 pixels will be collected within one word. The compact binary picture enables a quick image processing due to the very few bits actually set. It is estimated that a debris track can be initially identified within 30 to 40 ms.

Much more time-consuming is the masking process in the subframe generator where the target area for the next exposure is predicted. The new readout window must be wide enough to account for possible data scatter and guarantee a readable track length of at least 6 pixels in order to clearly distinguish from star images.

The star images are used for calibration purposes. The absolute intensity of the debris radiation must be determined with respect to the sensors response on the known brightness of selected stars. The size of the detected debris particles will then be calculated on the base of the more or less estimated albedo value and the range from the detector. The range /range-rate can only be determined from the subpixel interpolation of the moving debris image points on the CCD matrix in conjunction with the precise observation direction of the sensor in the inertial coordinate system. With a maximum relative misalignment of 5 arcsec. the range error will never exceed 10%. This high accuracy can only be achieved with an in-orbit calibration of the sensor orientation by means of an accurate star coordinate determination in pre-selected matrix windows. The focused star images should at least cover a 3 x 3 pixel field to enable subpixel interpolation.

The star selection and coordinate determination in the CCD matrix is time consuming and runs in parallel to the repeated debris track evaluations. Whereas track windows are taken from the binary picture the sensor system calibration is repeated after one or two seconds only. With the sensor proposed alignment calibrations it depends finally on the accuracy of the available orbit and attitude data of the carrying space vehicle how precise the orbital elements of the detected debris can be determined. Moderate accuracy for statistical applications can be achieved, even with elliptical debris orbits ($e < 0.1$), with the standard AOCS-error rates and merely 6 to 20 consecutive exposures per debris encounter.

5. IN ORBIT DEMONSTRATION

From our study (Ref. 8) point of view an on-orbit debris detector technology demonstration experiment can be realized in the near future with very moderate expenditures. Existing, space qualified hardware comprising optical components, focal plane/opto-electronical devices and the computerized image data processing units in principle have to be modified for the very special task.

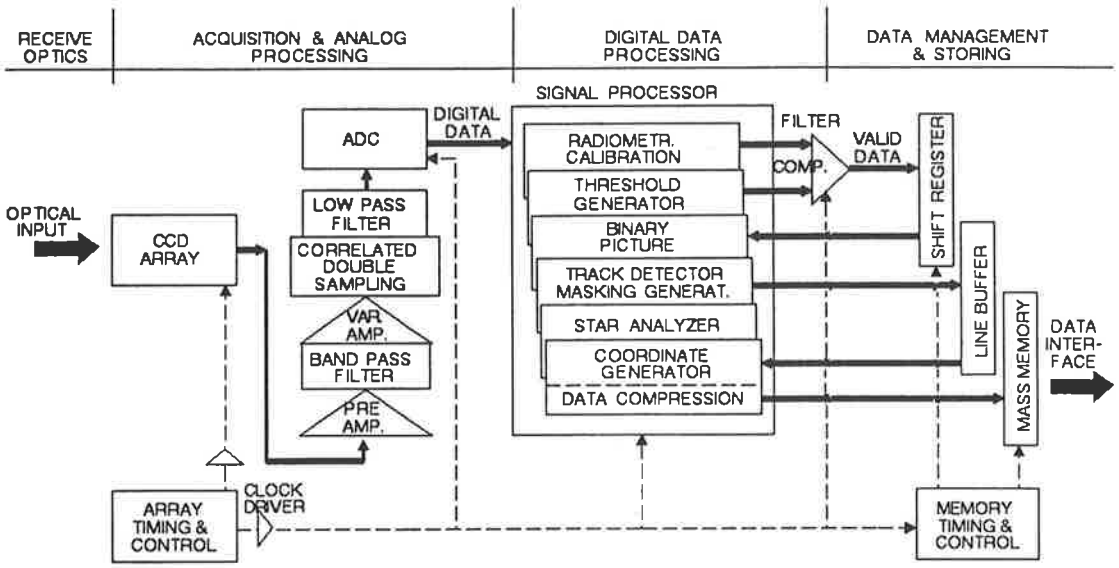

Figure 12. Functional diagram of proposed sensor electronics

Software conceptual work and feasibility check-up of the envisaged algorithms have already been started. However, the detailed specifications can only be established when the mission scenario and the experiment carrier with the dedicated subsystem/experiment interfaces are defined. The major objectives can be summarized as follows:

- to demonstrate in the near future with moderate expenditures the feasibility of optical debris detection in the visible spectral range
- to investigate principles of data acquisition and evaluate data storage/transmission requirements for advanced automated hardware
- to provide a set of debris flight path data which shall be utilized in order to control and probably modify the existing debris population models (e. g. ESA, NASA-models)

From various studies (Refs. 4, 9-11) it is revealed that the polar orbit within a certain eccentricity and with a telescope directed anti-solar provides the best conditions for debris monitoring. Such conditions would be found on the COLUMBUS polar platform (PPF) to be operational in 1998. However, from the experimental point of view a retrievable carrier or even better, a regularly surveyed experiment on board a space station with the capability to exchange and return data tapes to ground, are to be favoured. A space platform with planned astronomical missions in 1994 through '96 would be the retrievable STS/ Shuttle pallet ASTRO-SPAS (the SPAS-ORFEUS mission is currently under preparation). However, with a free flight phase of only a few days in a STS compatible orbit (i=28°, h=300 km) this carrier might not be suitable for debris detection.

So, it remains to be investigated in detail, if a technology experiment can be accommodated on the MIR1 station. ESA/DARA are planing COLUMBUS precursor experiments to be performed on MIR1 at least in two cooperative missions until 1996. Although MIR, from the debris monitoring point of view is at a too low orbit (app. 350 km), the relatively high inclination (51.6°) offers acceptable contrast and object illumination conditions. The relatively low event rate (app. 10 to 20% of the rates given in Fig. 7 for an 800 km orbit) in the achievable detection range can partly compensated by an extended experiment duration with data transfer during the regular servicing periods of the Russian space station.

The results of such an experiment (e.g. on board of MIR1) would be the bases for further activities , even if the detection scenarii of the mission does not match those of a 800 km sun-synchronous orbit. Most of the relevant parameters can be scaled. In terms of the achievable object illumination, such an orbit provides adequate conditions, if the right ascension during winter matches a specific window.

6. CONCLUSIONS

In addition of ongoing or planned ground-based debris measurements, which represent an important contribution for debris model validation within their capabilities, space based measurements have the capability to provide a significant in-situ impression of what orbital debris is about. The proposed procedures are in favour of such a capability and they allow for an in orbit debris detection experiment on the short term by the use of existing, space qualified components. Hence, the cost for such an experiment would be in a moderate regime. Based on such an experiment more advanced space based systems could be developed in order to monitor the in situ debris environment, e.g. at the altitude region of about 800 km, continuously.

7. REFERENCES

1. Space Station Freedom Program Office, *Space Station Program Natural Environment Definition for Design,* Revision A, SSP 30425, Reston/Virginia, 1991

2. Eichler P. and Rex D., *Study Report R8840,* Institute of Spaceflight Technology and Nuclear Reactor Technology, Technical University of Braunschweig, 1988

3. Levine A.S (Editor), *LDEF - 69 Months in Space*, NASA CP-3134, Proceedings of the 1st LDEF Post-Retrieval Symposium, Kissimee, FL, 1991

4. Reynolds R.C, et al.,Observing Orbital Debris using space-bases Telescopes: I. Mission Orbit Considerations, *Publication of the Astronomical Society of the Pacific* ,Vol. 101, p.1055-1060, 1989

5. Stansberry E. G., et al., Characterization of the Orbital Debris Environment using the Haystack Radar, *NASA Rep. JSC-32213*, Houston, TX, 1992

6. Henize K. G. and Stanley J., Optical Observations of Space Debris, *AIAA Orbital Debris Conference*, AIAA 90-1340, Baltimore, MD, 1990

7. Potter A.E., et al., Albedo Estimates for Debris, *Orbital Debris from Upper-Stage Breakup*, p.147-156, AIAA, Washington, DC, 1989

8. MBB ERNO, JENA OPTRONIK, DLR-IFA, IFRR TUBS, *Optical Debris Detection*, Final Report, DARA Contract no. 50 IP 9157, 1992

9. Neste S., et al., *Feasibility Study for Space Debris Detection Concepts*, General Electric, NAS9-16459, 1982

10. Nock K.T., A possible Small-Debris Monitor System, *Proc. First Conference on Space Debris,* Pasadena, CA, 1989

11. Eichler P., Bendisch J., Zhang J., Closing the Data Gap of Space Debris: Ground based or Space Based Sensors, *Proc. 4th European Aerospace Conference*, ESA SP-342, Paris, 1991